# Stability of subsea pipelines during large storms

Invited paper to Special Issue 'Advances in Fluid Mechanics for Offshore Engineering' of the Philosophical Transactions of the Royal Society, Part A.

23rd June 2014

**Scott Draper**
Assistant Professor
Centre for Offshore Foundation Systems
University of Western Australia
35 Stirling Hwy
Crawley, Perth, WA 6009
Australia
Tel: +61 (0) 8 6488 7400
Fax: +61 (0) 8 6488 1044
Email: scott.draper@uwa.edu.au

**Hongwei An, Liang Cheng**
School of Civil and Resource Engineering
University of Western Australia
35 Stirling Hwy
Crawley, Perth, WA 6009
Australia

**David J. White**
Shell EMI Chair
University of Western Australia
35 Stirling Hwy
Crawley, Perth, WA 6009
Australia

**Terry Griffiths**
Wood Group Kenny
Wood Group House
432 Murray Street
Perth, WA 6000

No. of words: 6200
No. of tables: 2
No. of figures: 16

## Abstract

On-bottom stability design of subsea pipelines transporting hydrocarbons is important to ensure safety and reliability, but is challenging to achieve in onerous metocean conditions typical of large (Tropical Cyclone/ Hurricane/ Typhoon) storms. This challenge is increased by the fact that design guidelines give no guidance on how to incorporate the potential benefits of seabed mobility, which can lead to lowering and self-burial of the pipeline on a sandy seabed. In this paper we demonstrate recent advances in experimental modelling of pipeline scour and present results investigating how pipeline stability can change in a large storm. An emphasis is placed on the initial development of the storm, where scour is inevitable on an erodible bed as the storm velocities build up to peak conditions. During this initial development we compare the rate at which near bed velocities increase in a large storm (on the order of $10^{-5}$ to $10^{-3}$ $m/s^2$) to the rate at which a pipeline scours and subsequently lowers (which is dependent on the storm velocities, but also on the mechanism of lowering and the pipeline properties). We show that these rates influence pipeline embedment during a storm and the stability of the pipeline.



**Keywords:** pipeline stability, scour, offshore hydrodynamics

## 1.0 Introduction

The lateral stability of subsea pipelines and cables in large storms is an important design requirement for oil and gas developments, and is also of importance for data communication infrastructure and marine renewable electricity networks. To ensure lateral stability in practice two approaches are commonly employed. Firstly the pipeline or cable self-weight maybe increased (known as primary stabilisation) with the addition of, for example, a concrete coating. Secondly additional means of stabilisation may be adopted (known as secondary stabilisation) which may include trenching, anchoring and/or rock dumping. Presently each of these approaches are known to provide reliable design solutions, but they come at a cost, with recent accounts suggesting that stabilisation comprises 30% of the cost of recent pipeline projects (Brown et al. 2002). This is a substantial amount given that the total capital cost of pipelines now exceeds $US4 million per kilometre of pipe (Randolph and Gourvenec 2011).

Primary and secondary stabilisation solutions are designed on the basis of conventional design approaches, incorporating industry guidelines such as DNV-RP-F109 (DNV 2010) and industry best practices (see, for example, Tørnes et al. 2010). However, it is widely accepted that these design approaches are incorrect and may be overly conservative on sandy seabed because they do not account for any variation in pipeline embedment following the initial placement of the pipeline. This approach is incorrect because the same wave and current velocities which are evaluated to assess pipeline stability will almost always have the potential to mobilise sediment on a sandy seabed well before they can mobilise the pipeline (Palmer, 1996). A more correct stability analysis must therefore account for scour of sediment from beneath the pipeline and the potential for pipeline lowering, which will alter pipeline embedment and have a direct impact on hydrodynamic loading and lateral soil resistance.

The detailed processes of pipeline scour and lowering have been described at length by Fredsøe et al. (1988) and Sumer and Fredsøe (1994, 2002) and are known to commence due to pre-existing gaps under the pipeline or when a scour hole initiates beneath a pipeline due to ‘piping’ (e.g. Chiew 1990) or, for example, due to variations in sediment supply (e.g. Zhang et al. 2013). The scour hole then tends to expand vertically beneath the pipe in a process known as tunnel erosion, which occurs at a rate that is dependent on the near seabed velocity, the pipeline geometry and the pipeline initial embedment (see Leeuwenstein et al. 1985, Sumer and Fredsøe 2002). The scour hole will also begin to extend along the pipeline at a rate which is dependent on these same parameters in addition to the three dimensional geometry of the scour hole and the span shoulders (Hansen et al. 1991; Cheng et al. 2009, 2013; Wu and Chiew, 2012).

At some point the scour hole(s) become sufficiently long that lowering of the pipeline occurs. In principle two mechanisms can cause this lowering (Figure 1). Firstly, if scour holes initiate at locations which are widely spaced along the pipeline (relative to a length $l_C = \left(100D \times EI/w'\right)^{1/4}$, where $D$ is the pipeline diameter, $EI$ is the bending stiffness of the pipeline and $w'$ is the submerged weight per meter length) the pipeline can 'sag' into the hole (Fredsøe 1988). Alternatively, if the scour holes are closely spaced (i.e. $l_{IP} < l_C$, where $l_{IP}$ is the spacing between initiation points of scour along the pipeline) then the pipeline can 'sink' into the supporting soil between spans when they become short (Sumer and Fredsøe 1994). Detailed analysis of pipeline field observations has identified both of these lowering mechanisms on the North West Shelf of Australia (Leckie et al. 2014).

Incorporating scour and pipeline lowering into stability design requires that the cumulative effects of scour can be estimated for all velocities contributing to sediment mobility prior to a stability analysis. In a large storm this therefore requires that scour associated with the storm velocities leading up to peak conditions is included in the analysis. This type of analysis leads to some general questions. Firstly, does the stability of a pipeline increase during the initial stages of a storm due to scour? And secondly, if the stability of a pipeline increases (continuously or eventually) with scour, can sufficient scour happen during the initial development of a storm to ensure stability? Or, put more simply, how do (i) the rate of scour and pipeline lowering and (ii) the rate at which near bed current and wave velocities increase in a typical storm, play-off to determine the stability of a pipeline?

The principle aims of this paper are to investigate aspects of these questions by building on previous literature which has focused mainly on scour in stationary (i.e. steady or periodically steady) velocities. Since scour and pipeline lowering during a storm is a problem of fluid-structure-seabed interaction that is difficult to model numerically, physical experiments have been performed in a large recirculating (O-Tube) flume using an actively controlled pipeline (see An et al. 2013 and Mohr et al. 2014 for more details). This facility is unique in that it can reproduce steady and oscillatory velocities which approach those measured and expected at the seabed during large storms, whilst simulating a section of pipeline free to translate (but not roll). The O-Tube facility has been constructed as part of the STABLEpipe JIP which has been undertaken to improve stability design of pipelines by accounting for the effects of sediment transport and scour.

The remainder of this paper is structured as follows. In Section 2 the rates at which near bed velocities increase in storms offshore North West Australia are reviewed based on available measurements. These rates are then used to provide the context for a series of experiments preformed in the O-Tube and described in Section 3 to measure variations in pipeline stability

during sagging and sinking due to scour in the development stage of a storm. Detailed results and analysis of these experiments are presented for sagging and sinking in Section 4 and Section 5. Discussion on the results is given in Section 6.

## 2.0 Storm development

In many offshore locations around the world extreme environmental loading conditions are dominated by rapidly rotating low pressure weather systems called cyclones (also called hurricanes in the North Atlantic and North East Pacific Oceans or typhoons in the North West Pacific Ocean). This is particularly true in North West of Australia, where approximately four to five cyclones occur during November to April each year (McConochie, 2010). These cyclones tend to generate in the warmer waters of the Arafura and Timor Seas, before travelling a few thousand kilometres in a west to south west direction over their lifetime (Hearn and Holloway, 1990). The intensity of a cyclone (which can be defined in terms of the maximum wind speed or pressure at the centre of the storm; Harper, 2002) and the direction (or track) can change continuously during its lifetime.

In intense cyclones (i.e. Category 4/5 or 5/5) offshore North West Australia significant wave heights can exceed 10 m, with the actual height being dependant on the central pressure in the cyclone, the geometry of the cyclone (often defined in terms of the radius to maximum winds) and the forward velocity of the cyclone (Young, 2003). In addition to increased waves, currents driven by the pressure and wind forcing associated with a cyclone can reach values in excess of 2 m/s near the water surface (Jonathan et al. 2012). This magnitude is a function of the intensity of the cyclone (through the pressure and wind forcing) and the storm track relative to the coastline and the underlying bathymetry (Hearn and Holloway, 1990; Zhu and Imberger, 1996).

To provide some insight into the development of these cyclonic storms Figure 3 reproduces surface wave measurements and current measurements obtained in ~125 m water depth on the North West Shelf of Australia at the North Rankin A (NRA) gas production platform operated by Woodside (this location coincides with a location of many pipelines). These measurements have been collated from a limited range of publications (cited in the figure captions). Cyclone storm tracks for each of these storm time series (obtained from BOM, 2014) are shown in Figure 4 and summary statistics are given in Table 1.

Figure 3 indicates that the significant wave conditions at NRA tend to develop over a period of ~ 12-36 hours. During this period the wave height increases continuously with a rate reaching approximately 0.3 m/hour to 1 m/hour in the 3-6 hours before peak conditions (Table 1). Assuming that subsurface wave velocity amplitude varies linearly with wave height, this indicates an increase in significant wave velocity amplitude of between $8x10^{-5}$ m/s$^2$ and $3x10^{-4}$ m/s$^2$.

The only current measurements in Figure 3 are for Cyclone Orson. It can be seen that these near surface currents oscillate prior to the arrival of peak wave conditions due to the semi-diurnal tide, but then accelerate at a maximum rate of around 0.25 m/s/hour (or $6.9 \times 10^{-5}$ m/s$^2$) close to peak storm conditions. Significant contributions to this rate occur due to the barotropic and baroclinic currents.

The ratio of steady current to wave velocity is important in assessing pipeline stability because it has a strong influence on pipeline hydrodynamics and scour (for example the equilibrium scour depth; Sumer and Fredsoe, 2002). Although little comparative data is available, it is well-known that near-bed wave-induced velocities will be greater as water depth decreases (Sarpkaya and Isaacson, 1981). This results in a general increase in the ratio of current to wave velocities with water depth.

In combination, the measurements in Figure 3 lead to several observations. Firstly, peak conditions occur after a finite ramp-up time and so there is always likely to be some time prior to peak storm conditions when scour can occur. Secondly, the acceleration associated with near bed velocities for a particular location appears to be dependent on a number of factors, including not only the cyclone intensity but also the storm track. For instance, the present measurements show that fast ramp-up rates are experienced at NRA both in large storms (Orson) and in smaller storms (Tiffany) that track differently towards NRA but at a similar forward speed. Thirdly, using NRA as a reference, the acceleration associated with the wave and current velocities appears to be on the order of $10^{-5}$ m/s$^2$ to $10^{-3}$ m/s$^2$. Accelerations below this range are clearly expected for lower intensity cyclones, or for cyclones tracking further from the design location. However, it seems unlikely that accelerations significantly higher than this range will occur (since these require an increase in wave height significantly above 3.6 m/hour). We will therefore adopt $10^{-5}$ m/s$^2$ to $10^{-3}$ m/s$^2$ as a reference for large storms in the remainder of this paper.

**Table 1: Summary statistics for the cyclone data given in Figure 3 and Figure 4.**

| Tropical Cyclone | Wave Height | | | | Currents | | |
|---|---|---|---|---|---|---|---|
| | Peak Hs [m] | Time to peak [hrs] | Maximum Rate | Period [s] | Peak [m/s] | Time to peak [hrs] | Maximum Acceleration |
| Orson | 10-12 | 24-36 | 0.85 m/hr | 9.1[(2)] | ~1.2 | 3-6 | 0.25m/s/hr |
| Olivia | 12-13 | 12-24 | 1 m/hr | 12-13[(3)] | - | - | - |
| Vance | 8-9 | 24-36 | 0.3 m/hr | 9-10[(4)] | - | - | - |
| Frank | 12-14[(1)] | 12-24 | 0.6[(1)] m/hr | -[(5)] | - | - | - |
| Tiffany | 8 | 12-24 | 0.8 m/hr | 8-9[(4)] | - | - | - |

Notes: (1) This is maximum rather than significant wave height. Buchan et al. (2002) suggest peak Hs was 7.3 m. (2) Zero-crossing period. (3) Spectral peak period. (4) Mean period. (5) Not specified.

## 3.0 Experiments performed in O-Tube facility

A series of 12 experiments are reported in this paper. The first 9 of these experiments investigate scour leading to the mechanism of sinking and the last 3 investigate scour leading to the mechanism of sagging. The key difference between the sagging and sinking experiments is that in the former the pipeline is actively load controlled (using the approach outlined in An et al. 2013) to set the self-weight of the pipe whilst allowing for horizontal and vertical translation. Consequently it is possible to model the pipeline sinking into the seabed due to scour and to capture stability directly, by allowing the pipeline to translate due to any hydrodynamic forcing that exceeds soil resistance. In contrast, for the sagging experiments the displacement of the pipeline is controlled so as to mimic vertical movement of a short section of pipeline down into the centre of a scour hole (i.e. point A in Figure 1). This sagging approach is similar to that used previously by Fredsøe et al. (1988).

The model pipeline used in the experiments is 196 mm in diameter and extends across the complete width of the O-Tube (see Figure 4). This diameter is close to 1:1 scale for smaller diameter pipelines and umbilicals used on the North West Shelf of Australia. Extrapolation above or below this diameter (so as to consider gas pipelines for example) could be undertaken using scaling arguments, but is not considered in the present paper. Consequently the metocean conditions and the accelerations observed in Section 2 are compared directly to the experimental results to estimate scour and lowering of a 196 mm pipeline in field conditions. The ability to model at close to 1:1 scale is a significant advantage of the O-Tube; current velocities in the present experiments, for example, go well above 2 m/s in current only conditions and reach a peak velocity of 1.5 m/s (with a 12 second period) in combined wave and current conditions.

The experimental setup used in all experiments is shown in Figure 4. The O-Tube working section is 1 m wide, 1 m high (above the un-scoured sand bed) and 17 m long. An Acoustic Doppler Velocimeter (ADV) was used to measure the velocity upstream of the pipeline, whilst a video camera was used to capture the scour profile. Measurements of pore pressure were made at 16 points around the circumference of the pipeline at the centre of the pipeline (see An et al. 2013), and these were integrated to determine the hydrodynamic drag and lift forces on the pipeline. Load cells mounted between the pipeline and the actuator arms were also used (see An et al. 2013). Artificial silica sand with average grain diameter ($d_{50}$) of 0.243 mm was used throughout. The grain size distribution of this sand is close to uniform and the relative density is $s$ =2.65.

Table 2 lists the 12 experiments performed. In the sinking experiments a focus is placed on understanding the effect on pipeline stability of the rate at which the storm velocities increase. Therefore the flow acceleration $a_s$ associated with currents and waves has been varied for two storm conditions which are believed to be representative of seabed storm conditions near NRA. These storms have $M$ equal to 0.5 and 1, respectively, where $M = U_c/U_w$ with $U_c$ the current velocity at 0.4 m above seabed (ASB) and $U_w$ the maximum wave velocity at 0.4 m ASB. The condition corresponding to $M = 1$ is representative of relatively deep water condition were amplification of wave velocities is minimal at depth but currents may still increase. The case of $M$ =0.5 includes both regular waves and currents and is modelled with a period of 12 s (similar to that observed for Cyclone Olivia, for example). The pipeline weight is set to $SG$=1.5 throughout and the initial pipeline embedment relative to the far field seabed $e_f$ has been varied across three values (see Figure 1 for definition of $e_f$). Pipeline bending stiffness is not relevant in the sinking experiments because it is assumed that scour holes are sufficiently close (as required for sinking) that curvature of the pipeline is minimal.

In the sagging experiments the only variable that is altered is the pipeline bending stiffness to submerged weight ratio $EI/w'$. As will be explained later, this ratio determines the speed at which the pipeline lowers into the centre of the scour hole. The focus of these experiments is therefore to investigate the effect on pipeline stability of the rate at which the pipeline lowers. The value of $10^4$ $m^3$ is typical of 200 mm diameter pipelines on the North West Shelf of Australia. The values of $10^1$ $m^3$ and $10^6$ $m^3$ are representative of a relatively 'flexible' and a 'stiff' pipeline, respectively.

In addition to the experiments outlined in Table 2, one supplementary experiment was performed to better explore sagging. This experiment is explained further in Section 5.

**Table 2: Experiments performed in the O-Tube.**

| Experiment | Mechanism | Flow condition | | Rate, $a_s$ [m/s$^2$] | $e_f/D$ [-] | Pipeline properties | |
|---|---|---|---|---|---|---|---|
| | | M [-] | Period [s] | | | $SG$ [-] | $EI/w'$ [m$^3$] |
| PRS-01 | Sinking | 1 | - | $2x10^{-3}$ | ~0 | 1.5 | - |
| PRS-02 | Sinking | 1 | - | $2x10^{-2.75}$ | ~0 | 1.5 | - |
| PRS-03 | Sinking | 1 | - | $2x10^{-2.5}$ | ~0 | 1.5 | - |
| PRS-04 | Sinking | 1 | - | $2x10^{-2}$ | ~0 | 1.5 | - |
| PRS-05 | Sinking | 1 | - | $2x10^{-3}$ | ~0.1 | 1.5 | - |
| PRS-06 | Sinking | 1 | - | $2x10^{-3}$ | ~0.2 | 1.5 | - |
| PRS-07 | Sinking | 0.5 | 12 | $2x10^{-3}$ | ~0 | 1.5 | - |
| PRS-08 | Sinking | 0.5 | 12 | $2x10^{-3.5}$ | ~0 | 1.5 | - |
| PRS-09 | Sinking | 0.5 | 12 | $2x10^{-4}$ | ~0 | 1.5 | - |
| PRS-10 | Sagging | 1 | - | $2x10^{-3}$ | ~0 | - | $1x10^{1}$ |
| PRS-11 | Sagging | 1 | - | $2x10^{-3}$ | ~0 | - | $1x10^{4}$ |
| PRS-12 | Sagging | 1 | - | $2x10^{-3}$ | ~0 | - | $1x10^{6}$ |

## 4.0 Pipeline Sinking

In experiments PRS-01 to PRS-09 the pipeline was placed on the seabed (at a particular embedment depth) and scour was observed at the edges of the pipeline as the current and wave velocities increased. Following this one of two outcomes was observed: (i) the storm velocities increased rapidly and were sufficient to move the pipeline laterally (i.e. the pipeline was unstable) before the pipeline lowered significantly due to scour, or (ii) scour continued to develop and propagated inwards towards the middle of the pipeline. The pipeline then began to sink vertically into the seabed due to its own weight and remained laterally stable over until it was completely buried.

Figure 5 presents two snap shots of Experiment PRS-04 consistent with the first of these two outcomes. This pipeline became unstable after only 50 seconds of a current increasing from zero at an acceleration of $2x10^{-2}$ m/s$^2$. Figure 6 presents snap shots for Experiment PRS-01, which modelled the same pipeline but in a current accelerating at $2x10^{-3}$ m/s$^2$, equivalent to the upper end of accelerations discussed in Section 2. In this experiment the outcome was of the second type noted above, with the pipeline sinking by more than one diameter. The scour process observed in PRS-01 was similar to that drawn in Figure 7, with scour developing first at the sides of the pipeline in the O-Tube and the propagating at some velocity $v_h$ towards the middle of the pipeline.

In combination the results in Figure 5 and Figure 6 demonstrate clearly how the rate at which the near-bed velocities increase can have a significant effect on the stability of the pipeline. A summary of the first six experiments in current only conditions is presented in terms of the initial and final digitised seabed profiles in Figure 8. For an initial far field embedment of zero, a 'critical' acceleration exists between $2x10^{-3}$ and $2x10^{-2.75}$ $m/s^2$. When the rate is lower than this critical value the pipeline experiences sufficient scour in the initial stages (less than 1 hour) of the storm to bury completely. In contrast, when the rate is higher than this critical value the pipeline is laterally unstable during the development of the storm.

For Experiments PRS-05 and PRS-06 the initial embedment of the pipeline was increased artificially at the start of each experiment by translating the pipeline laterally across the seabed several times with amplitude of movement equal to 1 pipe diameter. In both of these experiments subsequent lowering of the pipeline due to scour was delayed compared to Experiment PRS-01, which was conducted at the same acceleration but with no initial embedment. This delay is shown clearly in Figure 9 which presents the vertical displacement of the pipeline in time and the centroid of the pipeline as the pipeline lowers due to scour. The delay indicates that a higher velocity was required to initiate scour at the ends of the pipeline when the pipeline was more highly embedded and is consistent with the findings of Sumer et al. (2001) who show that the critical velocity to cause onset of scour due to piping increases with increased embedment. In the present experiments the pipeline was found to be stable in both PRS-05 and PRS-06, however the delay in the onset of scour due to increased embedment suggests that the critical acceleration is likely to reduce with pipeline embedment. This expected trend in the critical acceleration with embedment is indicated by the thick curved line in Figure 8.

Extrapolating the results from Figure 8 to predict the critical rate for pipelines with different diameter, weight or embedment requires that the mechanism of sinking (and in particular the effect of these parameters on the rate of sinking) is clearly understood. Sumer and Fredsøe (1994) suggested that pipeline sinking at a span shoulder can be explained as a continuous bearing failure of an equivalent rectangular footing. However, although Figure 9 indicates that the vertical lowering of the pipeline is similar to that shown by Sumer and Fredsøe (1994) the present experiments show two notable differences. Firstly, the vertical displacement of the pipeline in the present experiments is not smooth and continuous throughout, but instead includes small 'jumps' in vertical displacement. This is indicative of episodic 'collapse' of the span shoulder, rather than a continuous bearing failure. With each collapse the pipeline most likely experiences an increase in contact area with the shoulder following a period of rapid lowering (Luo, 2013). Unfortunately direct evidence of this collapse, or the bearing mechanism, could not be captured in the present O-

tube experiments. The only information available regarding the shoulder length was that it did not appear to exceed 200 mm once the pipeline started to sink (based on pore pressure transducer measurements spaced at 100 mm centres along the pipeline). This corresponds to a span to shoulder length ratio of 4:1. The second notable difference in Figure 9 is that lowering of the pipeline is associated with a movement upstream of the pipeline. This suggests that the bearing failure mechanism at the shoulder is not symmetric about the axis of the pipe.

Given the apparent complexity of the mechanism of pipeline sinking at the span shoulder we do not attempt to systematically investigate it in this paper. Instead the results in Figure 8 are presented on the qualification that they are an experimental 1:1 scale representation of a 196 mm pipe with scour initiation points spaced regularly at 1 m spacing. If this is representative of field conditions then it is apparent that the pipeline would be stable under ramping currents up to and including $2\text{x}10^{-3}$ m/s$^2$ (which is the upper end of what is observed in field conditions) when the initial embedment is less than $0.2D$. In situations where the pipeline has scour initiation points more widely spaced than 1 m, but still sufficiently close for sinking to be the main mechanism of lowering, the rate of lowering will be less than that observed in the O-tube experiments. Correcting the results in Figure 8 to account for this increased spacing (whilst maintaining all other pipeline and soil properties) needs to incorporate the additional time required for scour to propagate along the pipe (at a velocity $v_h$) until the shoulder length is similar to that observed in the experiment.

Figure 10 presents a summary for the final three sinking experiments PRS-07 to PRS09. In combined wave and current conditions it can be seen that, once again, there is a critical rate at which the pipeline is just stable. This is in the range of $2\text{x}10^{-4}$ m/s$^2$ to $2\text{x}10^{-3.5}$ m/s$^2$ and is noticeably lower than that for current only conditions owing to the higher forces associated with waves. Based on the results in Figure 10 it is apparent that a 196 mm pipeline with $SG$ =1.5, no initial embedment and scour initiation points spaced at 1 m centres would not be stable in a large storm having a rate higher than $2\text{x}10^{-4}$ m/s$^2$ and a period of 12 seconds (similar to cyclone Olivia).

## 5.0 Pipeline Sagging

For widely spaced scour holes the pipeline can sag into the centre of the scour hole. At any time the amount of sagging is related to the length of the scour hole, the flexural rigidity of the pipeline and the submerged weight of the pipeline. Assuming that at both ends of the scour hole the constraint on the pipeline is somewhere between fixed and pinned, Fredsøe et al. (1988) suggested that the vertical deflection of the pipeline can be given by:

$$z_p = \frac{3}{384}\frac{w' l_s^4}{EI}, \tag{1}$$

where $l_s$ is the length of the scour hole. Generally this length will vary in time according to:

$$l_s = v_h \times t, \tag{2}$$

where, as noted in Section 4, $v_h$ is the rate of scour along the pipeline. Cheng et al. (2009, 2013) have recently given empirical expressions to predict this rate in currents and collinear waves and currents, which is dependent on the free field seabed shear stress, the soil grain size, pipeline diameter, pipeline diameter and the wave and/or current direction. Combining (1) and (2) gives:

$$\frac{dz_p}{dt} = \frac{3}{384}\frac{w'}{EI}\frac{d}{dt}\{(v_h t)^4\}. \tag{3}$$

Experiments PRS-10 to PRS-12 have been undertaken to explore scour and the hydrodynamic forces on the pipeline as it lowers according to equation (3). In the experiments all parameters, including the flow acceleration, are kept constant except the ratio of pipeline bending stiffness to submerged weight. This is equivalent to varying the rate of vertical displacement or lowering of the pipeline whilst holding all other parameters constant. A similar approach to this was used by Fredsøe et al. (1988) to explore sagging under constant currents, although they modelled a pipeline that dropped at a fixed rate. Using the model pipe in the O-tube it is relatively easy to adopt the more appropriate rate due to equation (3) which varies in time due to scour along the pipeline.

Figure 11 presents the experimental results for PRS-10 to PRS-12, giving the calculated vertical displacement of the pipeline (worked out using $v_h$ from Cheng et al. 2009 and equation (3)) and the scour hole depth as a function of time. The experimental velocity time series is also shown. The point in time when the vertical displacement of the pipeline matches the scour hole depth signifies when the pipeline has 'touched down' into the scour hole. At this point (identified as a spike in the vertical force reading via the load cells) no further vertical movement of the pipeline was simulated in the experiment. In all three experiments backfill of the scour hole then commenced.

With respect to Figure 11 it is clear that the final burial depth differs significantly across the experiments. The most flexible pipeline drops fastest into the scour hole, but only reaches a depth of $0.58D$. In contrast the stiff pipeline drops later and over a longer period of time, leading to a final depth of $1.28D$. Consequently the potential changes to stability as a result of sagging are experienced faster for a flexible pipeline, but the extent of lowering and the potential for greater long term stability are larger for a stiffer pipeline.

The reason for the difference in final lowered depth across the three experiments is due to the fact that the vertical position of the pipeline has an effect on scour locally beneath the pipeline. This

interaction is clear in Figure 12 which presents the scour profile around the pipeline as it moves vertically into the scour hole; as the pipeline drops (but has not yet touched the bottom of the hole) the scour hole increases in depth and the side slopes become steeper and more symmetric. This increase in scour hole depth does, however, take time to realise. Consequently the stiffer pipeline, which drops more slowly into the hole, can generate additional scour and lower to a greater depth.

In the sagging experiments load control of the pipeline allowed stability of the pipeline to be observed directly, since translations of the pipeline were permitted during testing. In contrast, for the sagging experiments changes to stability can be partially interpreted through the influence of sagging on the hydrodynamic forces experienced by the pipeline. To explore this influence Figure 13 presents the lift and drag coefficients for Experiments PRS-10 and PRS-11 based on integration of the pressure transducers around the pipeline. Initially, prior to any scour, the lift and drag coefficients are both large and positive. However, following the start of scour (indicated by increasing $S/D$ in Figure 11), but prior to vertical movement of the pipeline, there is a gradual reduction in drag coefficient and the lift coefficient becomes negative. These trends in the drag and lift coefficient are similar to those reported by Jensen et al. (1990) using fixed seabed measurements and by Zhao and Cheng (2008) using computational fluid dynamics. It is noted, however, that the magnitudes of the present results are lower than these early studies. Finally, as the pipe begins to sag into the scour hole the drag force continues to reduce, whilst the lift coefficient becomes positive owing to the loss of flow beneath the pipeline. For completeness Figure 14 presents the scour profile observed in the present experiments with that modelled by Jensen et al. (1990) and simulated by Zhao and Cheng (2008) at four scour hole depths prior to vertical movement of the pipeline.

Comparing the two experiments in Figure 13 it is clear the stiffer pipe (RPS-11) eventually achieves a much lower drag force because it can sag to a greater depth. The rate at which the pipeline sags into the scour hole, and how this affects the scour process and the final lowered depth of the pipeline, is therefore of clear importance to assess stability for a sagging pipeline.

To better quantify how the rate at which the pipeline sags alters the scour process a supplementary experiment was performed in which the pipeline was held fixed above the seabed with a far field embedment of zero. Scour was then allowed to develop until equilibrium conditions were reached at a steady current velocity. Following this the pipeline was then dropped in discrete steps to vertical positions of $z_p/D = 0.2$, 0.33, 0.46, 0.58, 0.71 and 0.84. For each position scour was allowed to develop until equilibrium. Figure 15 summarises the results from this supplementary experiment in terms of the scour hole depth. Each vertical dashed line indicates when the equilibrium conditions were reached and the pipeline was lowered.

Two quantities are of interest in Figure 15: (i) the evolution in equilibrium scour depth $S_{eq}$ and, (ii) the rate of scour with vertical movement of the pipeline. The first of these quantities clearly increases as the pipe moves downwards. This increase in depth, relative to the depth for $z_p = 0$, is shown to agree very well in Figure 16 with the trend suggested by Sumer and Fredsøe (2002) based on results from Hansen et al. (1986). To investigate the second quantity the following expression has been fitted to each interval of the data in Figure 15:

$$S(t) = S_{eq}\left(1 - \exp\left(-\frac{t - t_0}{T}\right)\right), \tag{4}$$

where $T$ defines a time scale of scour and $t_0$ can be interpreted as an 'offset' in time required to ensure that (4) agrees with the measured scour depth at the start of an interval after the pipeline has been lowered. The form of (4) when $t_0 = 0$ is the same as that introduced by Fredsøe et al. (1992) to describe the scour hole development in steady currents for a pipeline with $z_p = 0$. Adequate fitting of (4) using the equilibrium scour depths in Figure 16 was achieved (see Figure 15) when using a single value of $T$ =350 s. For the first interval of $z_p/D = 0$ this result is slightly lower than a value of 540 s calculated according to the empirical formula suggested by Fredsøe et al. (1992).

The reasonable fit between (4) and the measurements in the supplementary experiment suggests that the scour development observed in Figure 11 might be well predicted for any pipeline vertical position using Equation (4). Pursuing this approach, the rate of change in scour hole depth for a sagging pipeline may be predicted according to

$$\frac{dS'}{dt} = \frac{S'_{eq}(z'_p)}{T}\exp\left(-\frac{t - t_0}{T}\right) = \frac{S'_{eq}(z_p) - S'}{T}, \tag{5}$$

where $S' = S/D$ and $z'_p = z_p/D$. In this expression the time scale has been assumed for simplicity to be independent of pipeline deflection, based on the limited data provide in the supplementary experiment, whilst the equilibrium scour depth has been assumed to vary slowly in time due to changes in pipeline position (as observed in Figure 16).

Equation (5) has been used to back calculate the scour depth in Figure 11 according to:

$$S'(t) = \int_0^t \left(\frac{S'_{eq}(z_p) - S'}{T}\right) dt, \tag{6}$$

where the equilibrium scour depth has been estimated according to the expression (indicated by the line in Figure 16):

$$S'_{eq} = 0.86 \times \exp(0.6 z_p), \tag{7}$$

and the time scale is calculated according to Fredsøe et al. (1992)

$$T = 0.65 \times \frac{D^2\theta^{-5/3}}{50\left(g(s-1){d_{50}}^3\right)^{1/2}}. \quad (8)$$

where $g$ is acceleration due to gravity and $\theta$ is the non-dimensional shear stress. The constant 0.86 in (7) equals the equilibrium scour depth measured in the supplementary experiment for $z_p = 0$ and the constant 0.65 in (8) is the ratio of time scale (350 s) in the supplementary experiment to that obtained using the formula given by Fredsøe et al. (1992) (540 s). The non-dimensional shear stress has been computed using the velocity at 0.4 m ASB assuming a logarithmic velocity profile and a bed roughness of $z_0 = d_{50}/12$.

Despite the limited verification, it is apparent in Figure 11 that Equation (6) does a remarkably good job at predicting the scour depth observed in the experiments both prior to any pipeline vertical displacement and during vertical displacement. Furthermore the point at which the predicted scour hole depth intersects the pipeline displacement (which defines the final lowered depth of the pipeline) agrees to within 10-20 %.

## 6.0 Discussion

In this paper we have presented experimental results at approximately 1:1 scale using a unique recirculating O-Tube flume to assess the stability of 196 mm pipeline during the development stage of a storm. Stability has been assessed directly for the case of a sinking pipeline, whilst hydrodynamic forces have been measured to interpret stability for a sagging pipeline. The experiments have focused on the rate at which the storm velocities increase (shown herein only for sinking pipelines) and the rate at which the pipeline lowers (shown herein only for sagging pipelines), and the effect that these rates have on stability of a pipeline on a mobile seabed.

Experiments concerning a sinking pipeline have shown that there is a critical acceleration which defines when the pipeline is laterally stable in a storm. For a 196 mm pipe with scour initiation points spaced at 1m centres along the pipeline the critical acceleration is between $2\text{x}10^{-3}$ m/s$^2$ and $2\text{x}10^{-2.75}$ m/s$^2$ in currents, and between $2\text{x}10^{-4}$ m/s$^2$ and $2\text{x}10^{-3.5}$ m/s$^2$ in combined waves and currents (with $M$ =0.5 and regular wave period of 12 seconds). These accelerations are similar to those observed offshore North West Australia. Extrapolation of the critical acceleration requires more detailed understanding of the sinking mechanism. However, it is expected that the critical acceleration will increase if pipeline SG increases (so that sinking can occur more quickly) and as the pipeline embedment reduces. Changes in the critical acceleration are also expected for different storm conditions, different soil and pipeline properties (i.e. diameter) and when the distance between scour initiation points changes.

In the case of sagging pipelines the rate of sagging has been shown to have a direct effect on the final lowered depth, in agreement with Fredsøe et al. (1988). For a 200 mm pipeline having a bending stiffness to weight ratio of $1x10^4$ $m^3$ the final lowered depth can exceed one diameter, which is much greater than the equilibrium scour depth without vertical movement of the pipe. Furthermore, as the pipe stiffness increases the lowered depth can increase further. Traditional design approaches which ignore scour, and consequently design to increase the weight of the pipeline (through the addition of armour wires for example) may therefore actually limit long term stability of the pipeline contrary to the design intention. For sagging pipelines we have also shown that a simple model of scour, which is applicable as the pipeline lowers, gives remarkably good agreement with experiments in current only conditions. This provides a valuable tool for estimating the scoured embedment and ultimately the stability in sagging. In future work this model can be used to assess the effect on pipeline sagging of the acceleration associated with the near bed velocities.

Collectively the results in this paper have demonstrated that scour can happen quickly in the development stage of a storm, leading to significantly different pipeline embedment in less than 1-2 hours for the 196 mm pipeline modelled. This time frame is within that observed for maximum acceleration in large storms and suggests that it is essential to account for scour on sandy seabed in large storms so as to correctly assess pipeline stability.

## Acknowledgements

The authors would like to thank Qin Zhang for Figure 4. The first author kindly acknowledges the support of the Lloyd's Register Foundation. Lloyd's Register Foundation helps to protect life and property by supporting engineering-related education, public engagement and the application of research. This research is also generously supported through ARC Discovery Grants Program: DP130104535.

## References

An, H., Luo, C., Cheng, L., and White, D. (2013) A new facility for studying ocean-structure-seabed interactions: The O-tube, *Coastal Engineering*, vol. 82, 88-101.

Bureau of Meteorology: http://www.bom.gov.au/

Buchan, S.J., Black, P.G. and Cohen, R.L. (1999). The impact of Tropical Cyclone Olivia on Australia's Northwest Shelf, *Offshore Technology Conference*.

Cheng, L., Yeow, K., Zhang, Z. and Teng, B. (2009), Three-dimensional scour below offshore pipelines in steady currents, *Coastal Engineering*, vol. 56, 577-590.

Cheng, L., Yeow, K., Zhang, Z. and Teng, B. (2014), 3D scour below pipelines under waves and combined waves and currents, *Coastal Engineering*, vol. 83, 137-149.

Chiew, Y. M. (1990). Mechanics of local scour around submarine pipelines, *Journal of Hydraulic Engineering*, vol. 116(4), 515-529.

Det Norske Veritas (NDV). (2010). On-bottom stability design of submarine pipelines, DNV-RP-F109.

Fredsøe, J. Hansen, E.A., Mao, Y. and Sumer, B.M. (1988). Three-dimensional scour below pipelines, *International J. Offshore Mechanics and Arctic Engineering*, vol. 110, 373-379.

Fredsøe, J., Sumer, B.M. and Arnskov, M. (1992). Time scale for wave/current scour below pipelines, *International J. Offshore and Polar Engineering*, vol. 2(2), 13-17.

Hansen, E.A., Staub, C., Fredsøe, J. and Sumer, B.M. (1991). Time development of scour induced free spans of pipelines, *10th Offshore Mechanics and Arctic Engineering Conference, ASME*, Stavanger, Norway, vol. 5, 25-31.

Hansen, E.A., Fredsøe, J. and Mao, Y. (1986). Two dimensional scour below pipelines, *5th Offshore Mechanics and Arctic Engineering Conference, ASME*, Tokyo, Japan, vol. 3, 670-678.

Harper, BA; Mason, LB and Bode, L. (1993). Tropical Cyclone Orson - a Severe Test for Modelling, *Australasian Conference on Coastal and Ocean Engineering*, Townsville, Qld.

Harper, B. A. (2002). Tropical cyclone parameter estimation in the Australian region-wind-pressure relationships and related issues for engineering planning and design-a discussion paper, SEA Rep. No. J0106-PR003E.

Hearn, C. J., & Holloway, P. E. (1990). A three-dimensional barotropic model of the response of the Australian North West Shelf to tropical cyclones, *Journal of Physical Oceanography*, vol. 20(1), 60-80.

Jensen, B.L., Sumer B.M., Jensen, H.R. and Fredsøe, J. (1990). Flow around and forces on a pipeline near a scoured bed in steady current. Trans, *J. Offshore Mechanics and Arctic Engineering*, vol. 112, 206-213.

Jonathan, P., Ewans, K., & Flynn, J. (2012). Joint modelling of vertical profiles of large ocean currents, *Ocean Engineering*, 42, 195-204.

Leckie, S.H.F., Draper, S., White, D.J. and Cheng, L. (2014). Lifelong embedment and spanning of a pipeline on a mobile seabed, Submitted to *Coastal Engineering*.

Leeuwenstein, W., Bijker, E.A., Peerbolte, E.B., and Wind, H.G. (1985). The natural self0burial of submarine pipelines. Proc. *4th International Conf. on Behaviour of Offshore Structures (BOSS)*, vol. 2, 717-728.

Luo, C. (2013). On-bottom stability of submarine pipeline on mobile seabed. PhD Thesis, University of Western Australia.

McConochie, J. D., Stroud, S. A., & Mason, L. B. (2010). Extreme hurricane design criteria for LNG developments: Experience using a long synthetic database. *Offshore Technology Conference*.

Mohr, H., Draper, S., Cheng, L., White, D., An, A. and Zhang, Q. (2014) 'The hydrodynamics of a recirculating (O-tube) flume', Submitted to *Continental Shelf Research*.

Palmer, A. (1996). A flaw in the conventional approach to stability design of pipelines. *Offshore Technology Conference*.

Randolph, M., & Gourvenec, S. (2011). Offshore geotechnical engineering. CRC Press.

Sarpkaya, T., & Isaacson, M. (1981). Mechanics of wave forces on offshore structures. Van Nostrand Reinhold Company.

Sumer, B.M. and Fredsøe, J. (2002). The mechanics of scour in the marine environment. World Scientific Publishing Co. Pty. Ltd.

Sumer, B.M. and Fredsøe, J. (1994). Self-burial of pipelines at span shoulders. *International J. Offshore and Polar Engineering*, vol. 4(1), 30-35.

Tørnes, K., Zeitoun, H., Cumming, G., & Willcocks, J. (2009). A Stability Design Rationale: A Review of Present Design Approaches. *28th International Conference on Ocean, Offshore and Arctic Engineering, ASME*, Honolulu, USA, 717-729.

Tron, S.M. and Buchan, S.J. (2002). Determination of Maximum Ocean Single Wave Height and its Associated Period, *Australian Meteorology and Oceanography Society Conference*, Melbourne, February 2002.

Wu, Y., & Chiew, Y. M. (2013). Mechanics of Three-Dimensional Pipeline Scour in Unidirectional Steady Current. *Journal of Pipeline Systems Engineering and Practice*, vol. 4(1), 3-10.

Young, I.R., 2003, A Review of the Sea State Generated by Hurricanes, *Marine Structures*, vol. 16, 201-218.

Zhang, Q., Draper, S., Cheng, L., An, H., & Shi, H. (2013). Revisiting the Mechanics of Onset of Scour Below Subsea Pipelines in Steady Currents. *32nd International Conference on Ocean, Offshore and Arctic Engineering, ASME*, Nantes, France.

Zhao, M. and Cheng, L. (2008). Numerical Modeling of Local Scour below a Piggyback Pipeline in Currents, *Journal of Hydraulic Engineering*, vol. 134, 1452-1463

Zhu, S., & Imberger, J. (1996). Computer-simulated current responses to cyclones on the North West Shelf of Australia, *Mathematical and computer modelling*, vol. 24(3), 93-115.

## Figures

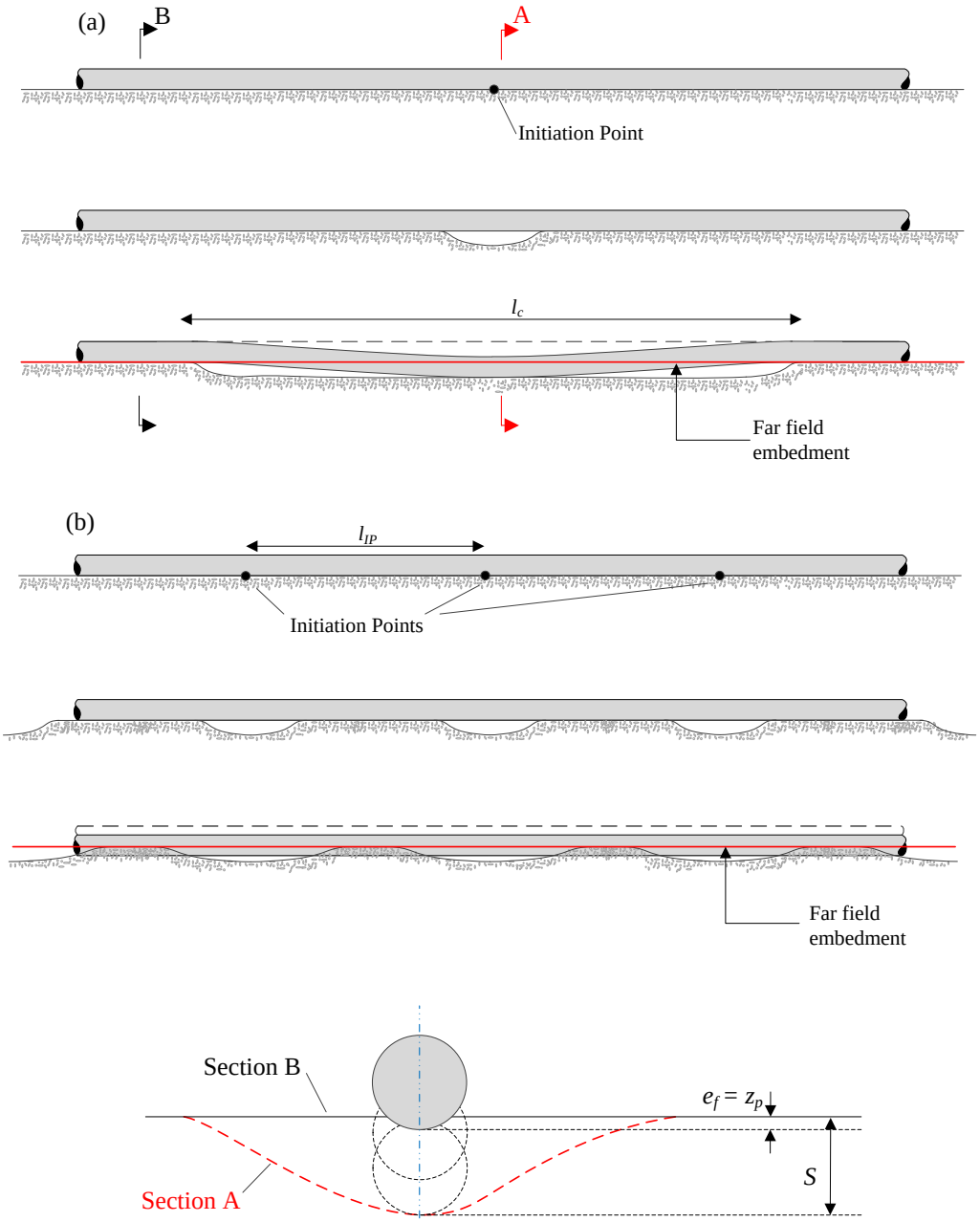


Figure 1: Mechanisms of pipeline lowering (a) via sagging into widely spaced scour holes, (b) via sinking into the supporting shoulders between closely spaced scour holes. Figure from Leckie et al. (2014).

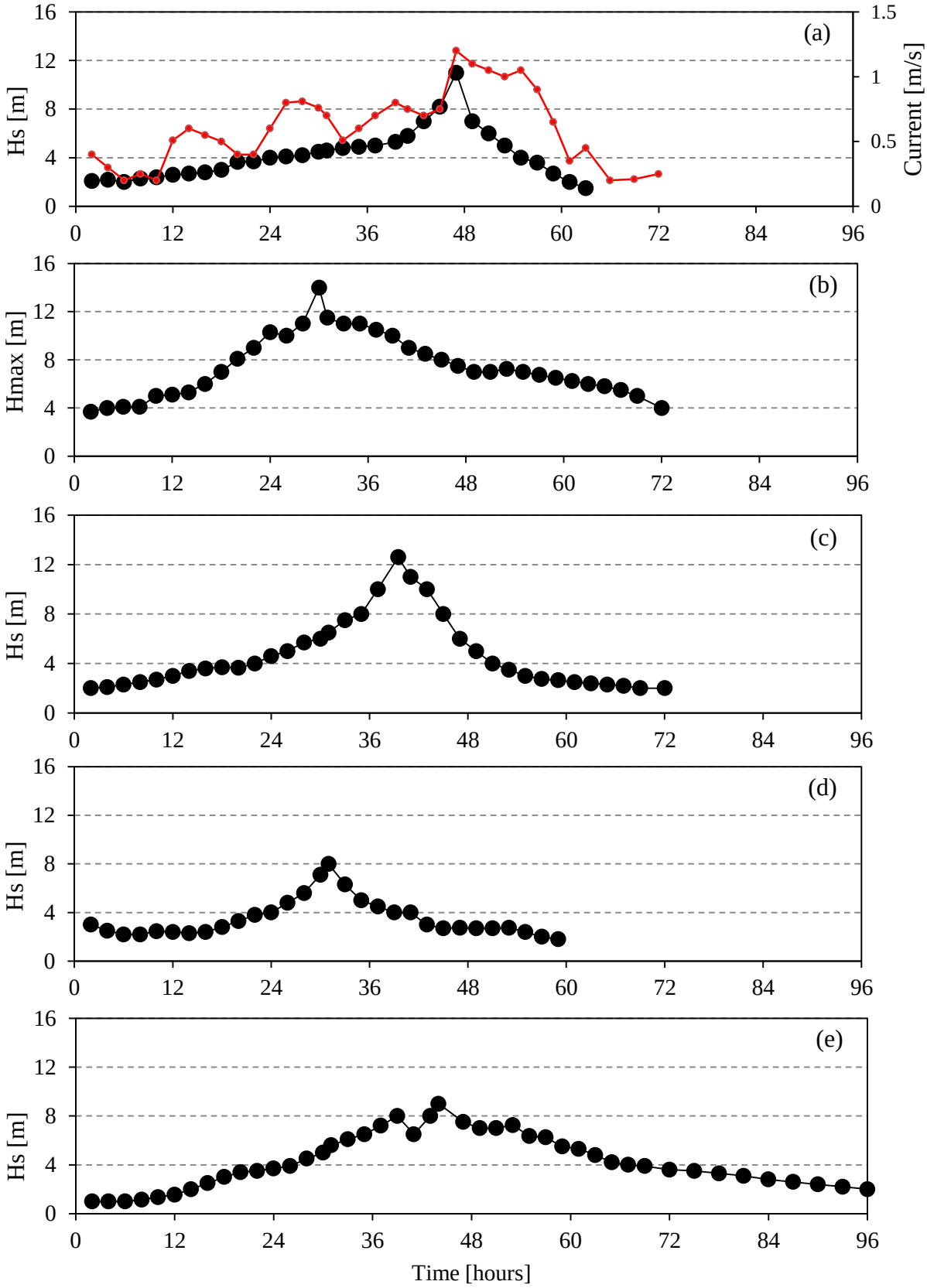


Figure 2: Time series of wave height and current (thin line only for case (a)) at NRA for five Tropical Cyclones. (a) TC Orson 1989 (b) TC Frank 1995; (c) TC Olivia 1996; (d) TC Tiffany 1998; (e) TC Vance 1999. Data in (a) from Harper et al. (1993), data in (c) from Buchan et al. (1999), data in (b) – (e) from Tron and Buchan (2002).

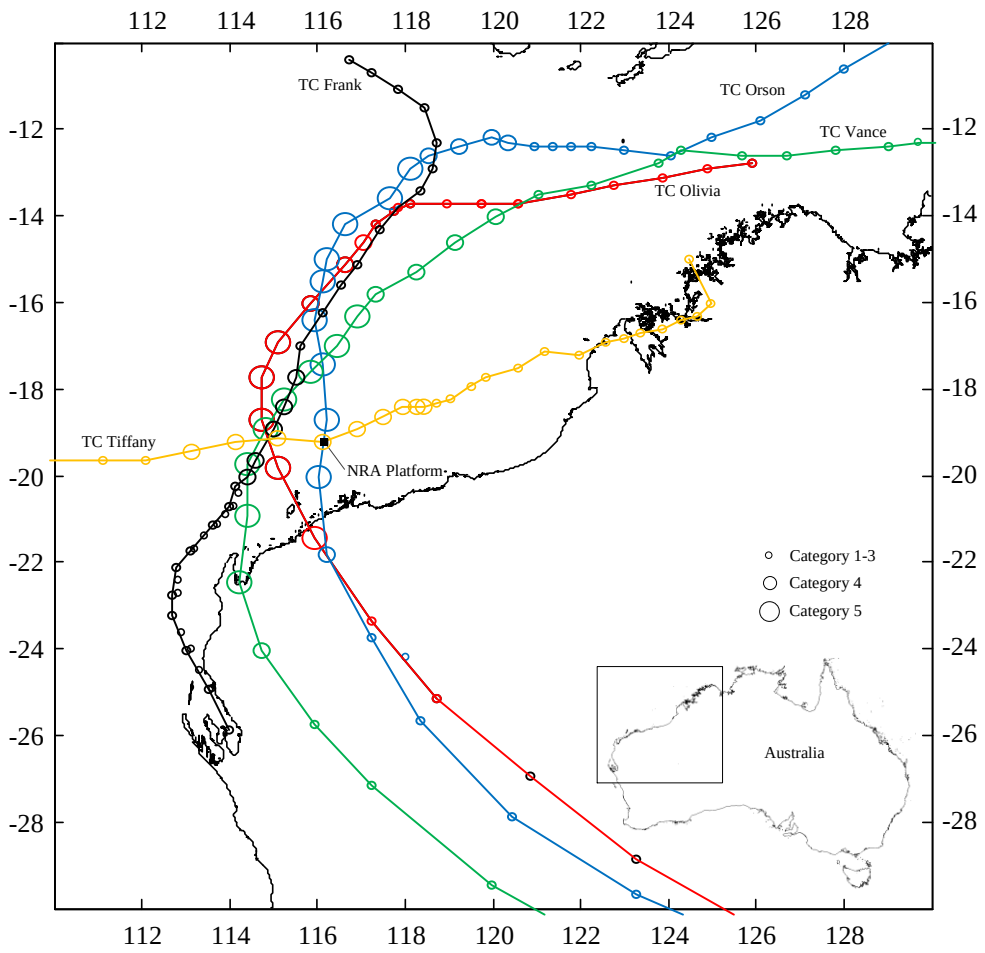


Figure 3: Cyclone tracks corresponding to storm time series given in Figure 2. Circles represent location of cyclone every 6 hours.

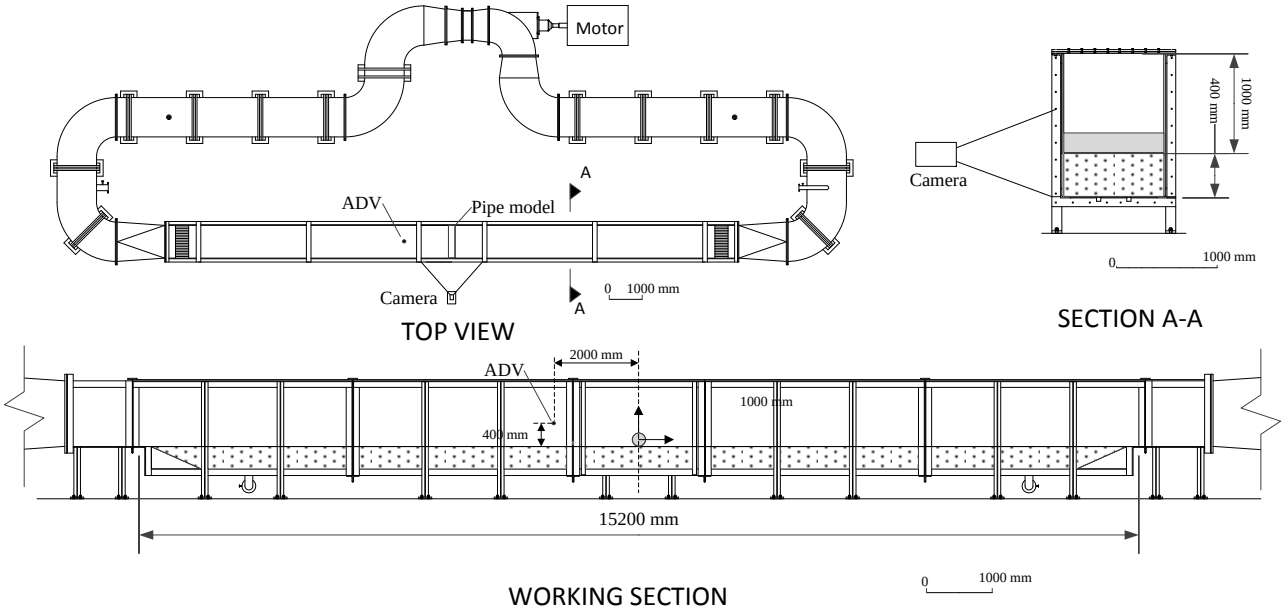


Figure 4: Large O-tube indicating location of pipeline and approximate location of camera.

(a) (b)

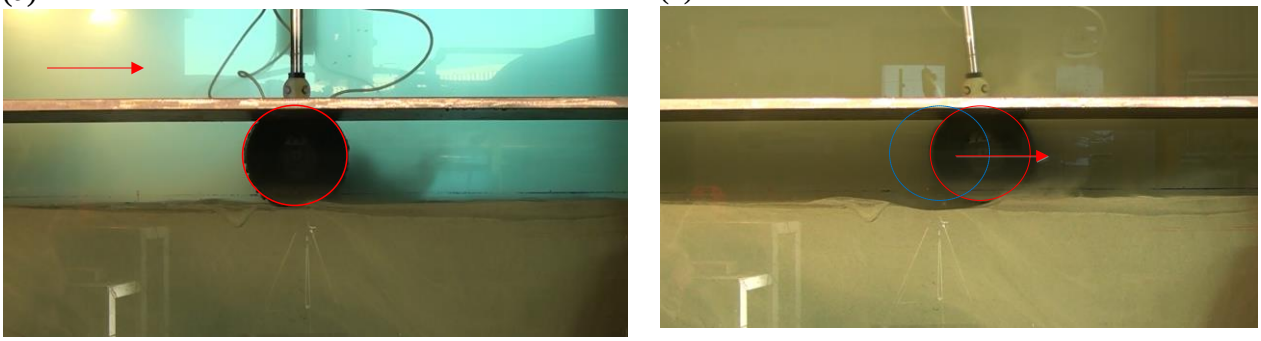

Figure 5: Two snapshots of PRS-04. The pipeline moved laterally before experiencing significant scour. Blue circle indicates initial location of the pipeline. Red circle identifies pipeline. Current si from the left.

(a) (b)

(c) (d)

(e) (f)

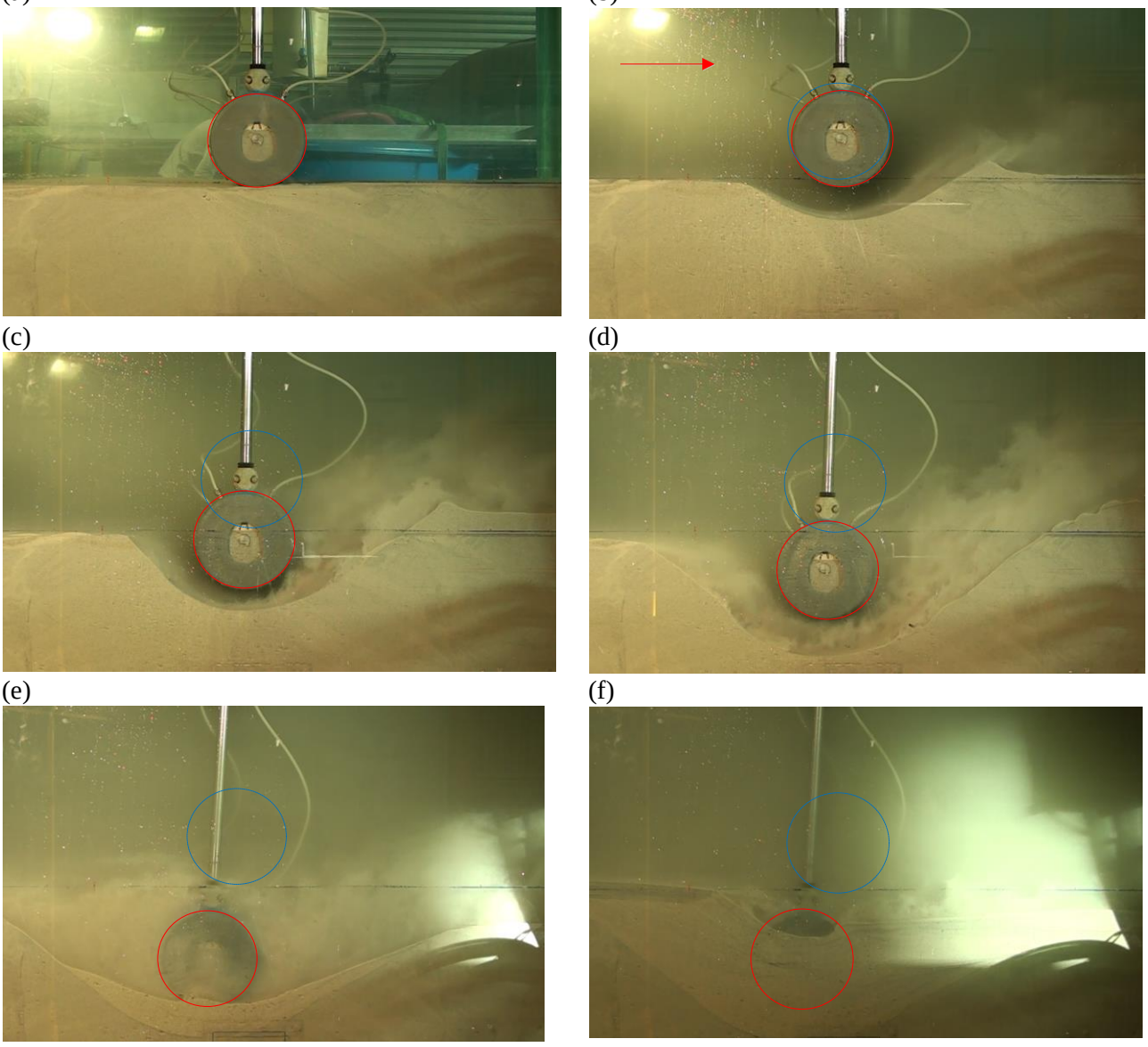

Figure 6: Six snap shots of PRS-01 showing pipeline sinking into the seabed. Blue circle indicates initial location of the pipeline. Red circle identifies pipeline. Current is from the left.

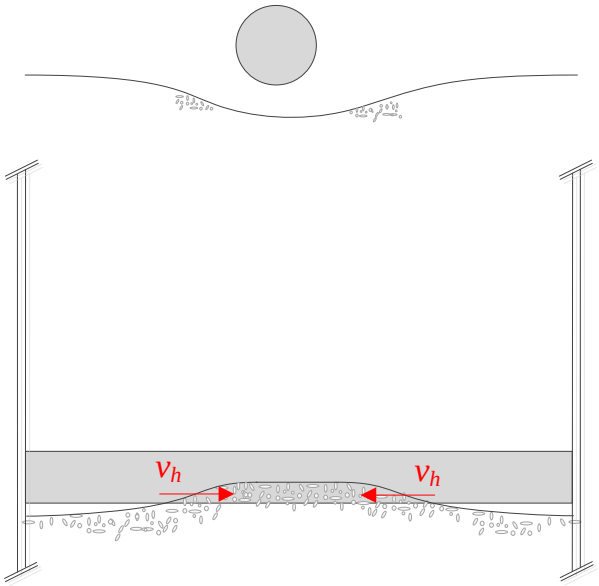


Figure 7: Scour profile along the model pipeline in the O-Tube.

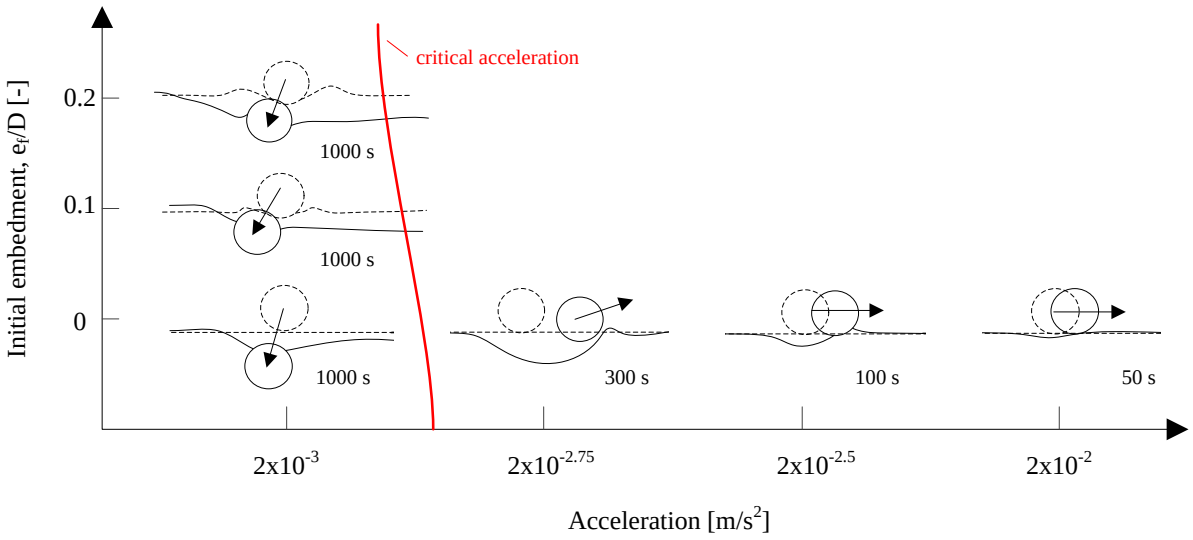


Figure 8: Digitised profiles at the end of experiment or at the point the pipe becomes unstable. The time for either of these two outcomes is written next to each figure. A critical acceleration is indicated, below which the pipeline is stable. Data is for current only.

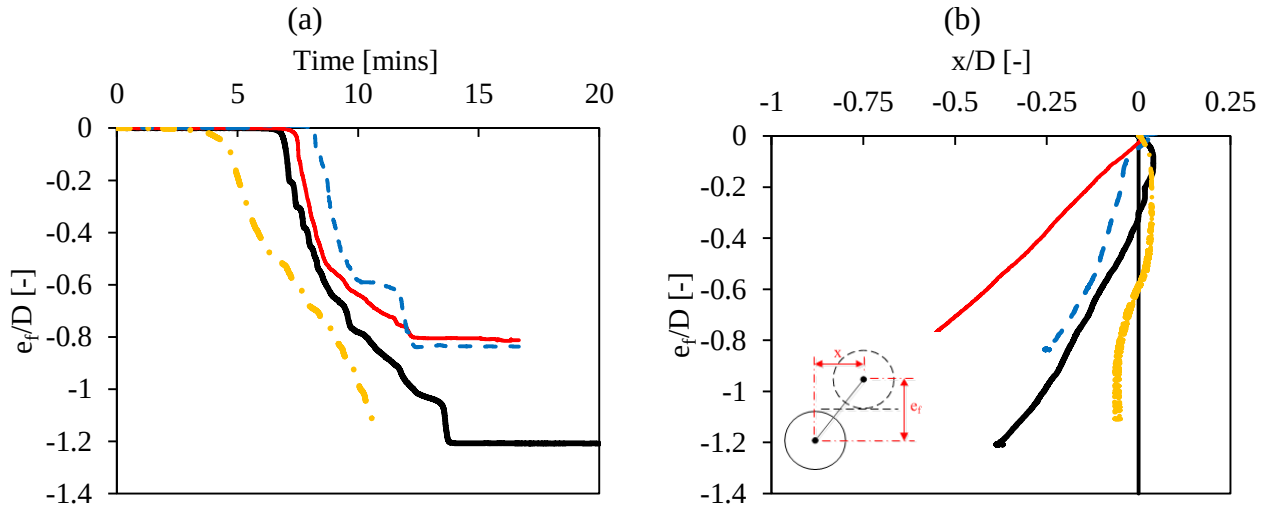


Figure 9: (a) Vertical displacement of pipeline during scour. (b) Translation of pipeline during scour (positive x-axis is aligned with mean flow direction). Thick black line is Experiment PRS-01. Thin red line is Experiment PRS-05. Dashed line is Experiment PRS-06. Chained orange line is Experiment PRS-09.

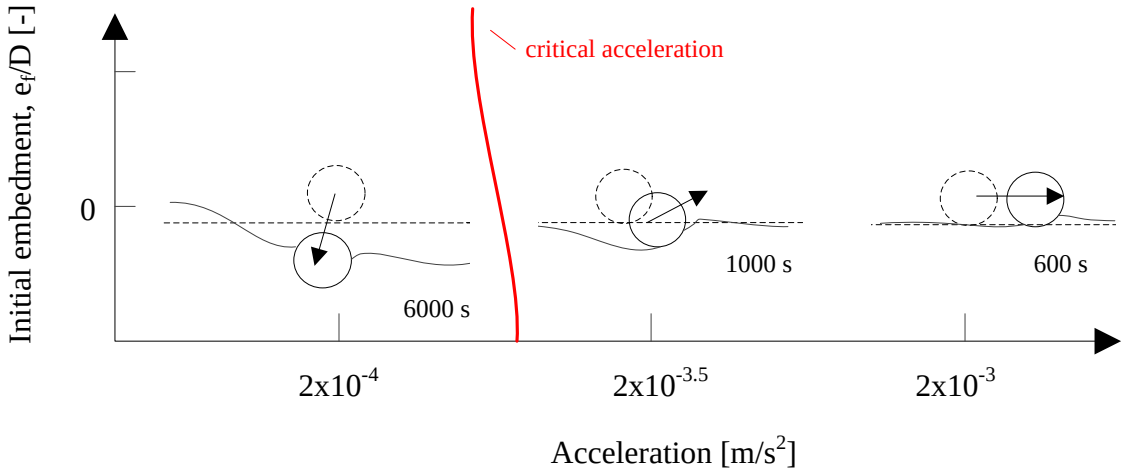


Figure 10: Digitised profiles at the end of experiment or at the point the pipe becomes unstable. The time for either of these two outcomes is written next to each figure. A critical acceleration is indicated, below which the pipeline is likely to be stable. Data is for combined wave and current conditions.

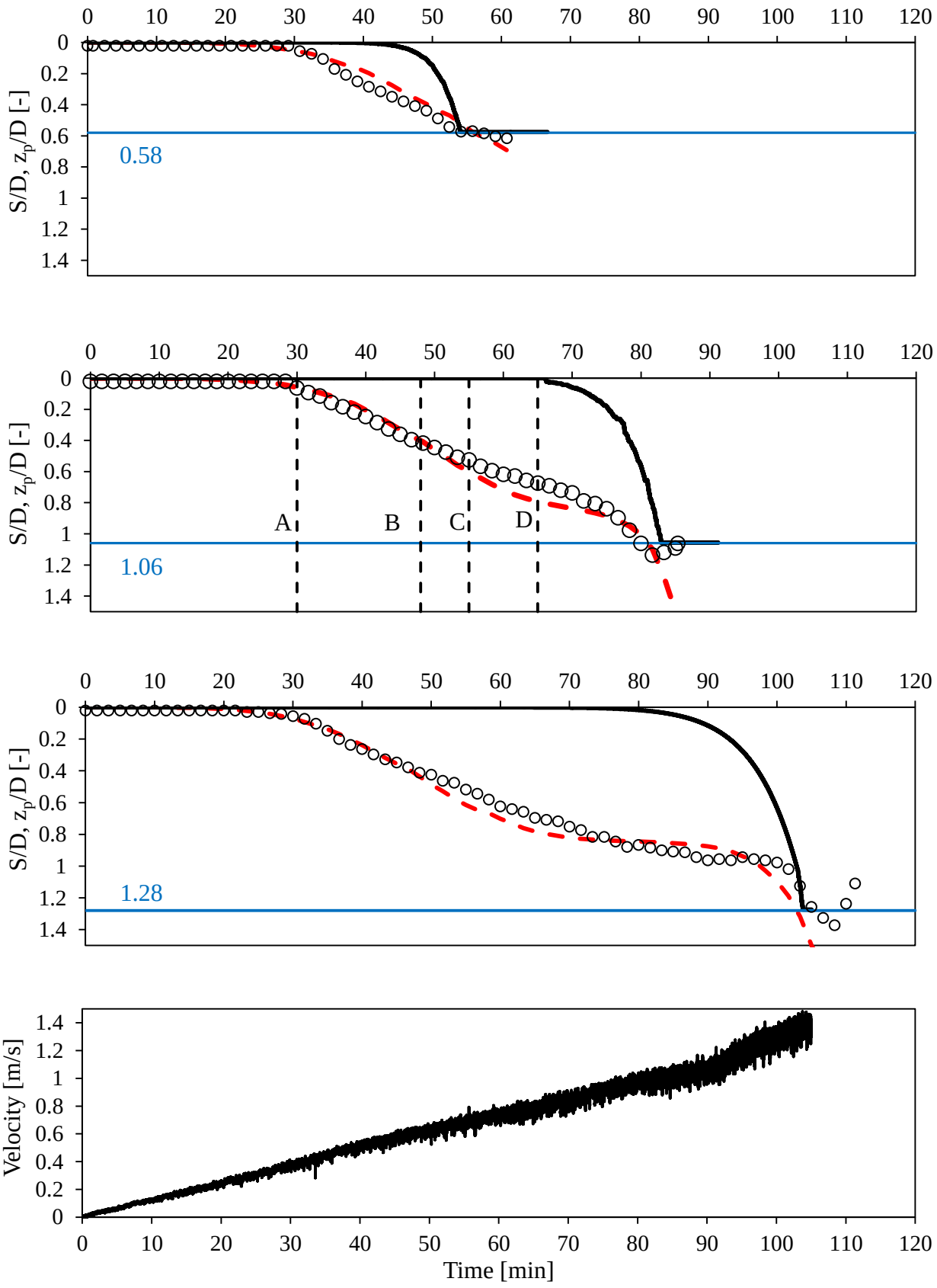


Figure 11: Variation in scour depth and pipeline position with time. (a) PRS-10; (b) PRS-11; (c) PRS-12. Solid dark line is the location of the bottom of the pipeline, *z*, circles are measured scour hole depth beneath the pipe, and solid sashed line is prediction from Equation (6).

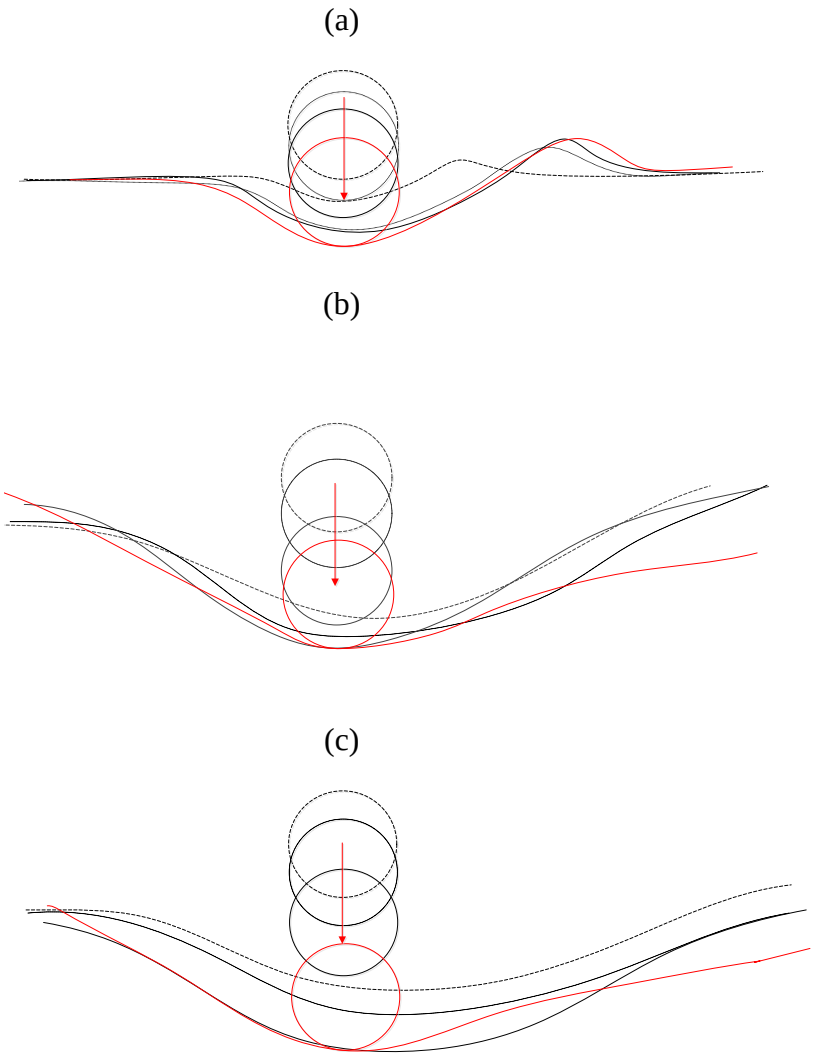


Figure 12: Variation in scour profile as pipeline sags into scour hole. (a) PRS-10, (b) PRS-11 and (c) PRS-12. Current is from the left.

(a)

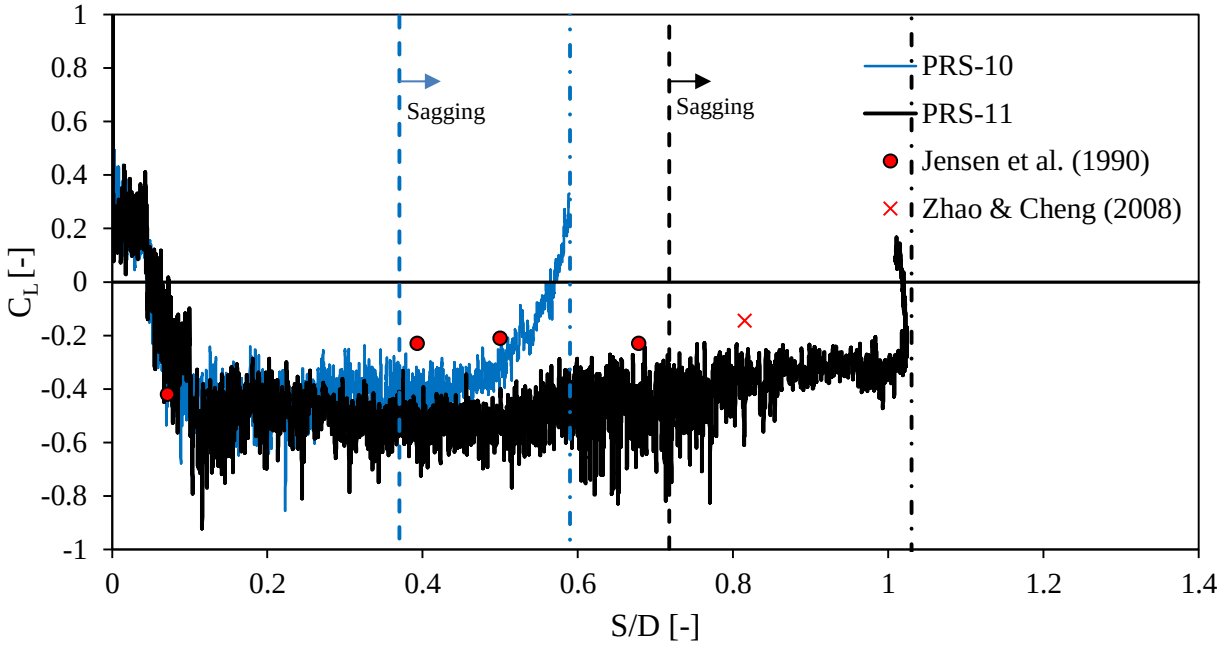


(b)

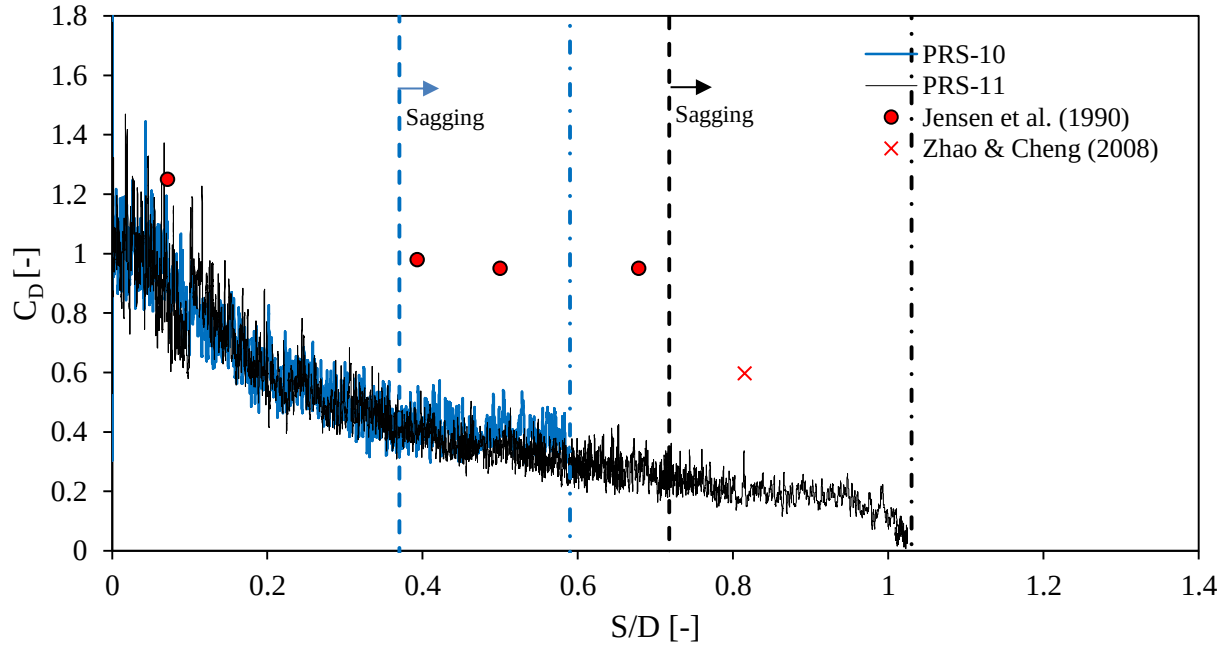


Figure 13: (a) Lift and (b) drag coefficients for experiments PRS-10 and PRS-11 as a function of scour depth. Lift and drag coefficients reported by Jensen et al. (1990) and Zhao and Cheng (2008) also shown.

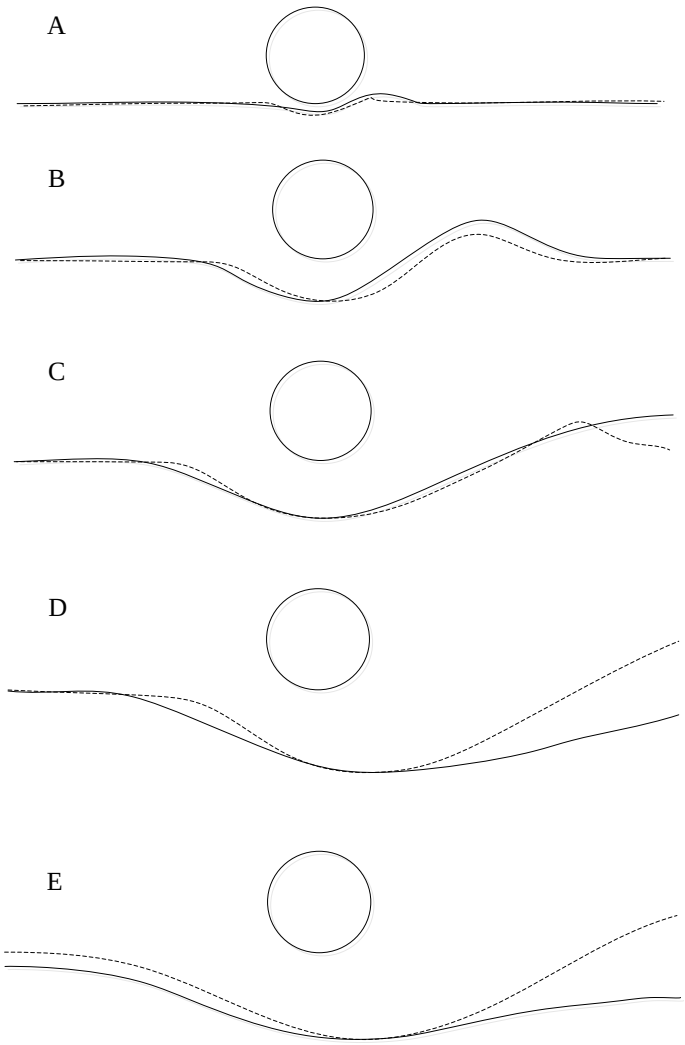


Figure 14: Profiles during the initial phase of scour (prior to pipeline movement). Dashed lines are digitised profiles from Experiment PRS-11. Solid lines in A to D are from Jensen et al. (1990) profiles II-V. Solid line in E is from Zhao and Cheng (2008). Current is from the left.

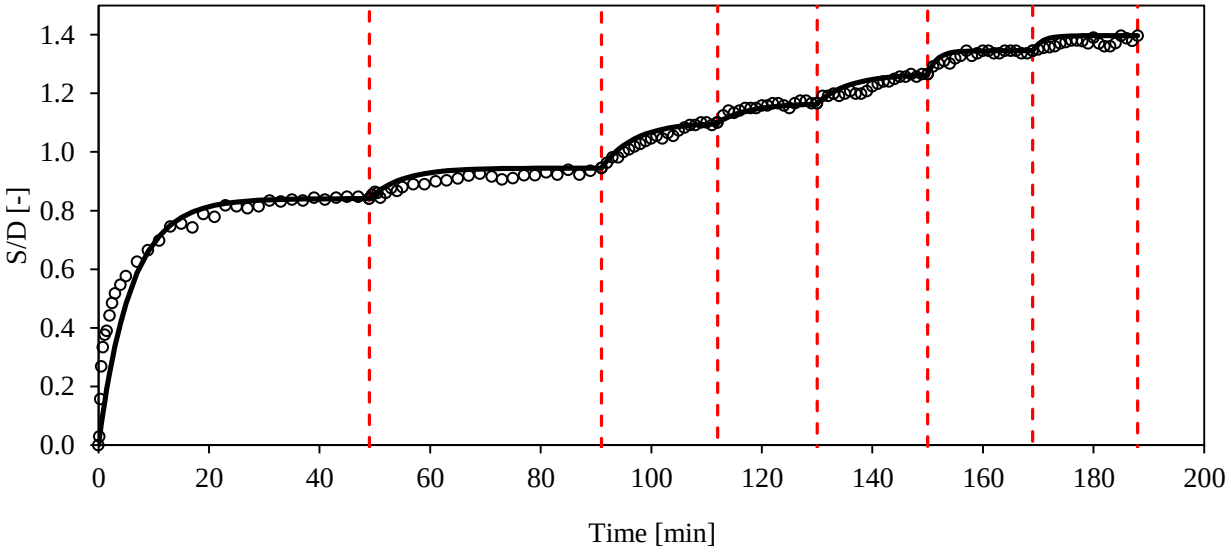


Figure 15: Development of scour hole depth for various pipeline positions given by $z_p/D = 0$, 0.2, 0.33, 0.46, 0.58, 0.71 and 0.84. Measurements are circle markers. Vertical dashed lines separate intervals where the pipeline had a different vertical position. Solid line is fit based on Equation (4).

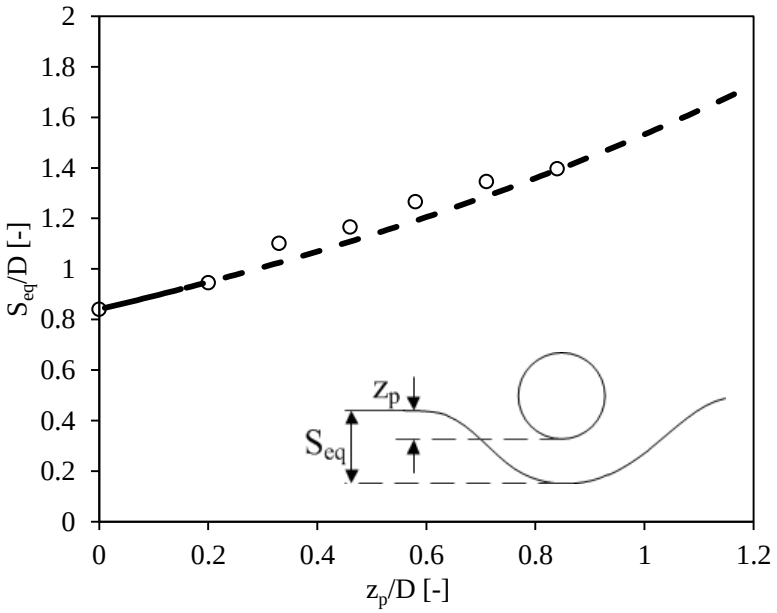


Figure 16: Variation in equilibrium scour depth as a function of pipeline far field embedment. Line indicates empirical expression for the multiplier on equilibrium scour depth without initial embedment (i.e. $e_f = z_p = 0$) due to Sumer and Fredsøe (2002) based on the results of Hansen et al. (1986). The dashed portion is outside the limits of that tested by Hansen et al.